Characterization of Phase Space Topology Using Density: Application to Fault Diagnostics

Mohsen Samadani[1], Cedrick A. Kitio Kwuimy[2], and C. Nataraj[3]

[1,2,3] *The Villanova Center for Analytics of Dynamic Systems (VCADS)*
Department of Mechanical Engineering, Villanova University, Villanova, PA, 19085, USA
msamadan@villanova.edu
cedrick.kwuimy@villanova.edu
nataraj@villanova.edu

ABSTRACT

Almost all engineered systems are nonlinear and show nonlinear phenomena that can only be predicted by nonlinear models. However, the application of model-based approaches for diagnostics has been constrained mostly to linearized or simplified models. This paper introduces a fundamental approach for characterization of nonlinear response of systems based on the topology of the phase space trajectory. The method uses the density distribution of the system states to quantify this topology and extracts features that can be used for system diagnostics. The proposed method has been employed to diagnose a multi degree of freedom system with various simultaneous defects.

1. INTRODUCTION

The ability to determine the state of the system and predict failures would greatly increase the safety and productivity of systems. The predictive maintenance, health monitoring and diagnostics methods have become the focus of many research projects in recent years (Rezvanizaniani, Dempsey, & Lee, 2014; Fekrmandi, 2015). Generally speaking, a defective system would have a different dynamical response from a healthy system. From the mathematical point of view, these dynamical changes can be caused by either alternations in the values of the system parameters or transformation of the structure of the model, which we would call parametric and structural defects, respectively. The development of a crack in a beam is an example of parametric defects which will result in a change in the stiffness of the beam. In contrast, structural defects cause change the structure of the mathematical model. A broken capacitor in an electrical circuit drops the first order derivative in the model and can be considered as a structural defect. Given the mathematical model of the system along its parameter values, one can easily obtain the response of the system using numerical integration techniques. In contrast, the diagnostics problem would be the inverse problem, where we have the dynamical response of the system and we want to identify and quantify changes in the mathematical model. The solution to this problem however, is not always a straight-forward task. In practice, all engineering systems are nonlinear and exhibit nonlinear phenomena that can only be predicted by nonlinear models. This includes periodic, multi-periodic, quasi-periodic and chaotic behaviour, limit cycles, bifurcations of the equilibrium points, etc. Many studies have reported the emergence of these complex nonlinear phenomena in machinery originating from defects or even due to their nonlinear nature in healthy conditions (Sankaravelu, Noah, & Burger, 1994; Mevel & Guyader, 1993; Kappaganthu & Nataraj, 2011). The prevailing estimation methods which are mostly based on optimization algorithms show poor performance coping with such complexities. In many cases, the models are linearized to simplify the estimation problem or behaviour of the system in such complex regimes is simply ignored.

A phase space is a space in which all states of a system are represented and a phase portrait is a visual representation of the trajectory of this space. For the two-dimensional case, the phase space will turn into a phase plane. The phase space trajectory consists of a closed single loop for a periodic response and multiple loops for a multi-periodic behaviour. The topology of the phase space trajectory provides valuable information regarding the dynamics of a system in a qualitative fashion. While much work has been devoted to extract information from these topological patterns (Letellier et al., 1995; Carroll, 2015; Tufillaro et al., 1991), the concern here is to extract a set of features that can quantify the phase space topology in order to do the inverse problem.

This paper presents a novel method for characterization of the nonlinear response of the system based on the topology

of its phase space. In an earlier work (Samadani, Kwuimy, & Nataraj, 2015), we developed a method that we name here "Phase Space Topology (PST)" for characterizing the topology of the phase space trajectory with quantitative measures. This method which is based on the probability density distribution of time series was used to extract features from the phase plane response of a 1-DOF nonlinear pendulum in the periodic and multi-periodic domains and estimate two parameters of the system. The present paper is an extension to the previous work which generalizes the applicability of the method to multi degree of freedom systems with higher complexities. A 3-DOF nonlinear mass-spring-damper system with up to six simultaneous parametric defects has been used for the demonstration of the method. The robustness and sensitivity of the characterization method to various parameters including noise, time series length and time step and density estimation parameters have been considered as well.

The rest of this paper is organized as follows. Section 2 provides an overview of the method of PST and the computational approach which has been used in this study. In section 3, the case study and its mathematical model are introduced. Section 4 describes the feature extraction and diagnostics procedure and presents the results of its application to numerical and experimental data. The conclusion has been presented in Section 5.

2. CHARACTERIZATION OF SYSTEMS USING THE METHOD OF PHASE SPACE TOPOLOGY (PST)

PST quantifies the topology of these closed curves by computing the density distribution of points along each axis of the phase space. For simplicity of illustration, the examples here are presented in the two dimensional space; however, it can be extended to higher dimensions. For dimensions higher than three, even though the visualization of the phase space space trajectory is not possible, the method is still applicable. In fact, the computations are performed individually and independently for each state of the system. The density of each state is computed by Kernel density estimator as described in the following

Kernel density estimation: Let X=(x_1,x_2,...,x_n) be an independent and identically distributed sampled data drawn from a distribution with an unknown density function f. The shape of this function can be estimated by its kernel density estimator.

$$\hat{f}_h(x) = \frac{1}{nh}\sum_{i=1}^{n} K\left(\frac{x - x_i}{h}\right) \tag{1}$$

where, h >0 is a smoothing parameter called bandwidth and $K(.)$ is the kernel function which satisfies the following requirements.

$$\int_{-\infty}^{\infty} K(u)\mathrm{d}u = 1 \tag{2}$$

$$K(-u) = K(u) \text{ for all values of } u \tag{3}$$

There are a range of kernel functions that can be used including uniform, triangular, biweight, triweight, Epanechnikov, normal, etc. Due to its conventional mathematical properties, we use the normal kernel function in our approach.

This density function can be computed and plotted for any state of the system. It turns out that the shape of the phase space trajectory which is a closed curve for periodic and multi-periodic behavior is in a direct relationship with the properties of the peaks in the density plots. Specifically speaking, as shown in (Samadani et al., 2015):

- At the end of the curve in the phase plane (where the curve turns back at the local maximum or minimum along each axis) the density of points is significantly higher than the other areas. This produces a sharp peak in the probability density plot of the corresponding axis. In other words, each loop in the phase plane portrait produces two sharp peaks in the density plot of each axis.
- The density of points on the curve at sharper ends (curvature with lower radius) is higher than density of points at rounder ends (bigger radius). Therefore, the sharper the end of the curve, the higher the corresponding peak will be in the probability density plot.
- A depression in the curvature of the phase plane causes a higher density of points in that region which is proportional to the extremeness of the depression and this creates a smooth peak in the probability density plot.

According to these empirical rules, the topology of the phase space trajectory can be characterized with the properties of the peaks in the density plot which themselves can be quantified with following measures:

- l_i : Location of the peaks
- h_i : Height of the peaks
- s_i : Sharpness of the peaks
  - Sharpness is defined as the difference between the left and right slopes at the peak

Therefore, the m dimensional trajectory of the phase space is mapped into m density plots, each of which containing several peaks whose properties can characterize the original trajectory. This mapping is unique for a specific set of estimation parameters; however, the inverse statement is not always true. In other words, there can be an unlimited number of phase space topologies for a given set of peak features. Let us now consider the phase plane portrait of a system response with n=30,000 sampled points shown in Fig. 1a. The data has been obtained by numerical integration of a second order ODE with time step Δt=0.001 sec. A closed curve with two

loops represents a bi-periodic behavior with two commensurable frequencies. The kernel density of the horizontal axis x evaluated at n_p=1000 points is shown in Fig. 1b, when h=5e-04 has been used for the kernel bandwidth value. As can be seen, the ends of the curve along the horizontal axis x has produced fours sharp peaks in the density plot. The curve has a lower radius in the left side than in the right side and therefore, the first peak in the density plot is higher and sharper than the last peak. The two peaks in the middle are also the result of the small loop in the middle of the phase plane. Similarly, due to the lower radius curvature in those turning points, their corresponding peaks are higher and sharper than the other two.

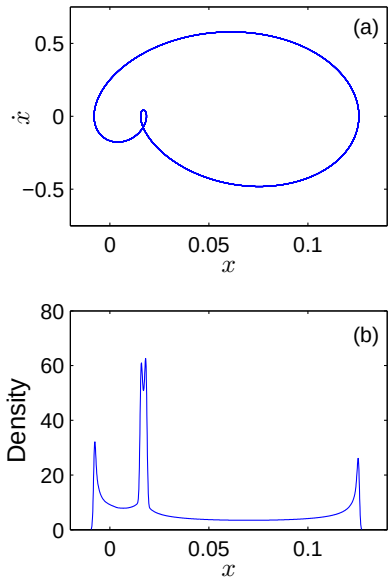

Figure 1. (a): A sample phase plane plot of a nonlinear second order system obtained from numerical integration (b): The distribution curve

3. CASE STUDY: DIAGNOSTICS OF A 3-DOF NONLINEAR OSCILLATOR WITH SIX PARAMETRIC DEFECTS

3.1. Experimental setup

A 3-DOF nonlinear mass-spring-damper system has been used in this study to demonstrate the implementation of the method. This system which is shown in Fig. 2a is a model 210-rectilinear plant manufactured by ECP and is designed to emulate a broad range of real-world applications including 1-DOF rigid bodies, flexibility in linear drives, gearing and belts, and other coupled discrete oscillatory systems. The mechanism consists of three mass carriages interconnected by springs. The mass carriages are mounted on anti-friction ball bearing type linear motions. Dashpots which provide adjustable viscous damping can be attached between the masses and the base

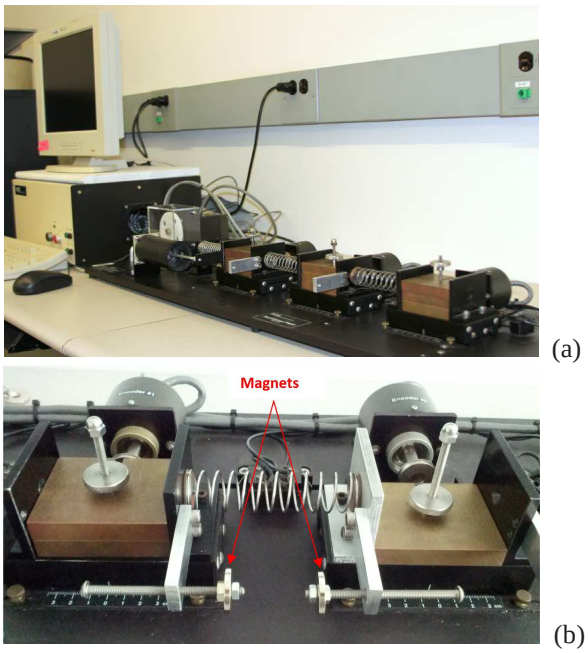

(a)

(b)

Figure 2. (a): Model 210-Rectilinear Apparatus. (b): Permanent magnets were used to produce nonlinear force and damping

plate. The position of all masses are measured by high resolution encoders. The masses, the springs stiffness and viscous damping of dashpots are adjustable and the reconfigurable design of the electromechanical apparatus allows the user to transform it into a variety of configurations which represent various important classes of real life systems. The rotary motion produced by a brushless DC servo motor is transformed to a linear excitation and is transmitted to the first carriage through a rack and pinion mechanism.

Model 210-rectilinear plant is originally a linear system. The system was transformed into a nonlinear mass-spring-damper system with mounting permanent magnetic discs on each mass carriage, as shown in Fig. 2b. With identical poles of magnets facing each other, a nonlinear repelling force is produced which is proportional to the inverse of the distance squared. In addition to this nonlinear force, a damping force is also produced by the magnets whose coefficient was found to be proportional to the inverse of the distance of magnets. The design of the system allows the user to adjust the initial distance of the magnets by rotating the screws on which the magnets are mounted.

3.2. Mathematical Model

The mathematical model of the system can be described by Eqn. 4. In this equation, $m_i, i = 1, 2, 3$ are the total mass of moving masses (The mass of carriages $m_c, i = 1, 2, 3$ plus the additional weights on each carriage), $k_i, i = 1, 2, 3$ are

the stiffness of springs, $c_i, i = 1, 2, 3$ are the viscous damping coefficients of each mass, c_m is the damping coefficient due to magnets, p is a constant coefficient associated with the force between magnets, $r_{0i}, i = 1, 2, 3$ are the initial distance of the magnets on each two masses, and μ is the coulomb friction coefficient.

The rated values of the parameters representing the system in healthy conditions were estimated using system identification techniques. The value of p was estimated by measuring the static force between two repelling magnets at different distances. The values of m, k and c were estimated by fitting the numerical response to the experimental initial condition response of each mass using the method of nonlinear least squares. This procedure was done for several times, and the average values of each parameter were obtained. The magnets then were attached to the mass carriages and the additional damping coefficient value added to the system due to the magnets were estimated. The estimated parameters of the system are presented in Table 1. Note that the second and third mass carriages are similar; therefore, their masses and damping coefficients are identical. Also, the same springs and magnets were used for all masses of the system.

The magnitude of the input force is adjusted by parameter A on the experimental setup. The relation of A and f_0 was obtained by scaling the amplitude of a periodic numerical response to fit the experimental response of the system. This relation was found to be:

$$f_0 = 6.4\ A \tag{5}$$

3.3. System diagnostics using PST

3.3.1. Feature extraction

This section demonstrates the implementation of the method of PST in order to estimate up to six parameters of the system including the values of the masses and initial distance of magnets. Due to the complexity of the system, if the range of parameters is not bounded, a variety of different behaviours can be seen in the system response. However in practice, the parameters of a system stay in a limited range in defective conditions. Here we assume that $m_i \in$ [0.8 1.0] kg and $r_{0i} \in$ [0.019 0.023] m for i=1,2 and 3. Figure 3 shows three sample phase portraits of the first mass response (position x_1 vs. velocity x_2) along with the corresponding density plots for both x_1 and x_2, for system parameters presented in Table 2.

Let us now see how the density of x_1 and its peaks properties change based on the topology of the phase portraits. In Fig. 3a, we have a double-loop phase portrait which is a characteristics of a bi-periodic motion. The edges of the loops in the x_1 direction have produced four sharp peaks in the density plot of x_1. The two sharp peaks in the middle are higher than the other two due the lower radius of the phase plot curve in those parts. In addition, the depression of the phase plane curve in the middle has produced a smoother peak in the density plot. In Fig. 3b we have a similar topology; however, the depressed part has moved rightward. It can be seen from the corresponding density plot that the smooth peak has shifted rightward to the middle of the two sharp peaks as well. In Fig. 3c another loop has been evolved in the phase plane; representing a response with three frequencies. As a result, two more sharp peaks have been emerged in the density plot of x_1. The density plots of x_2 can also be explained in a similar way. Although here we characterized the topology of the phase portrait of the first mass response based on the density of its position and velocity, this distinction between the system states is not always easy or practical as they can be of different natures (e.g position, velocity, electrical current, fluid flow, etc.). However, this process can be done for any state of the system independently; regardless of the nature or number of states. In other words, we do not even need to obtain any phase plots to do the analysis and the presented examples are just for the sake of illustration.

3.3.2. The inverse problem

With the features extracted from the states of the system, a machine learning tool can be used as a classifier to classify the faults or as a regressor to estimate the parameters of the system. An artificial neural network (ANN) has been used in this study to regress the computed features to the six parameters of the system. For this purpose, a two-layer feed-forward network with sigmoid hidden neurons and linear output neurons was developed. Due to the complexity of the system response and having three degrees of freedom, we will have a relatively large number of features for each sample of data. This requires a higher number of hidden neurons in order for the network to be trained with minimum regression error. The regression error was found to be minimum for twenty hidden neurons in this case. Depending on the number of the loops and the complexity of the curvature in the phase portrait, the number of peaks and therefore the number of inputs to the neural networks can vary. In this problem, we know that the maximum number of peaks is seven for the possible range of parameters. This knowledge can be obtained from bifurcation diagrams or by simulation of the system for many random parameter sets. We then build the matrix of inputs with respect to this maximum number. For example, in this problem, the response can produce a maximum of seven peaks. Three features are extracted from each peak and therefore, the number of inputs would be 21 for each state and 126 in total for all six states. For cases where the response of the system contains less number of peaks, since we need a constant number of inputs for the neural network, we choose to put zeros in the remaining columns, according to the procedure explained in (Samadani et al., 2015). The data was obtained by random selection of the values of parameters, simulation of the sys-

$$
\begin{aligned}
\dot{x_1} &= x_2 \\
\dot{x_2} &= \tfrac{1}{m_1}\left[f_0\sin(\omega t) + \tfrac{p^2}{(r_{01}+x_1)^2} - \tfrac{p^2}{(r_{02}+(x_3-x_1))^2} + k_2(x_3-x_1) - k_1x_1 - (c_1+c_m)x_2 - \mathrm{sign}(x_2)\mu m_1 g\right] \\
\dot{x_3} &= x_4 \\
\dot{x_4} &= \tfrac{1}{m_2}\left[\tfrac{p^2}{(r_{02}+(x_3-x_1))^2} - \tfrac{p^2}{(r_{03}+(x_5-x_3))^2} + k_3(x_5-x_3) - k_2(x_3-x_1) - (c_2+c_m)x_4 - \mathrm{sign}(x_4)\mu m_2 g\right] \\
\dot{x_5} &= x_6 \\
\dot{x_6} &= \tfrac{1}{m_3}\left[\tfrac{p^2}{(r_{03}+(x_5-x_3))^2} - k_3(x_5-x_3) - (c_3+c_m)x_6 - \mathrm{sign}(x_6)\mu m_3 g\right]
\end{aligned}
\tag{4}
$$

Table 1. Nominal parameter values of the nonlinear oscillator

m_{c1} (kg)	m_{c2} (kg)	c_1 (Ns/m)	c_2 (Ns/m)	k_1 (N/m)	p^2 (Nm^2)	c_m (Ns/m)	r_0 (m)
0.880	0.397	2.5	1.175	368	0.052	0.014	0.022

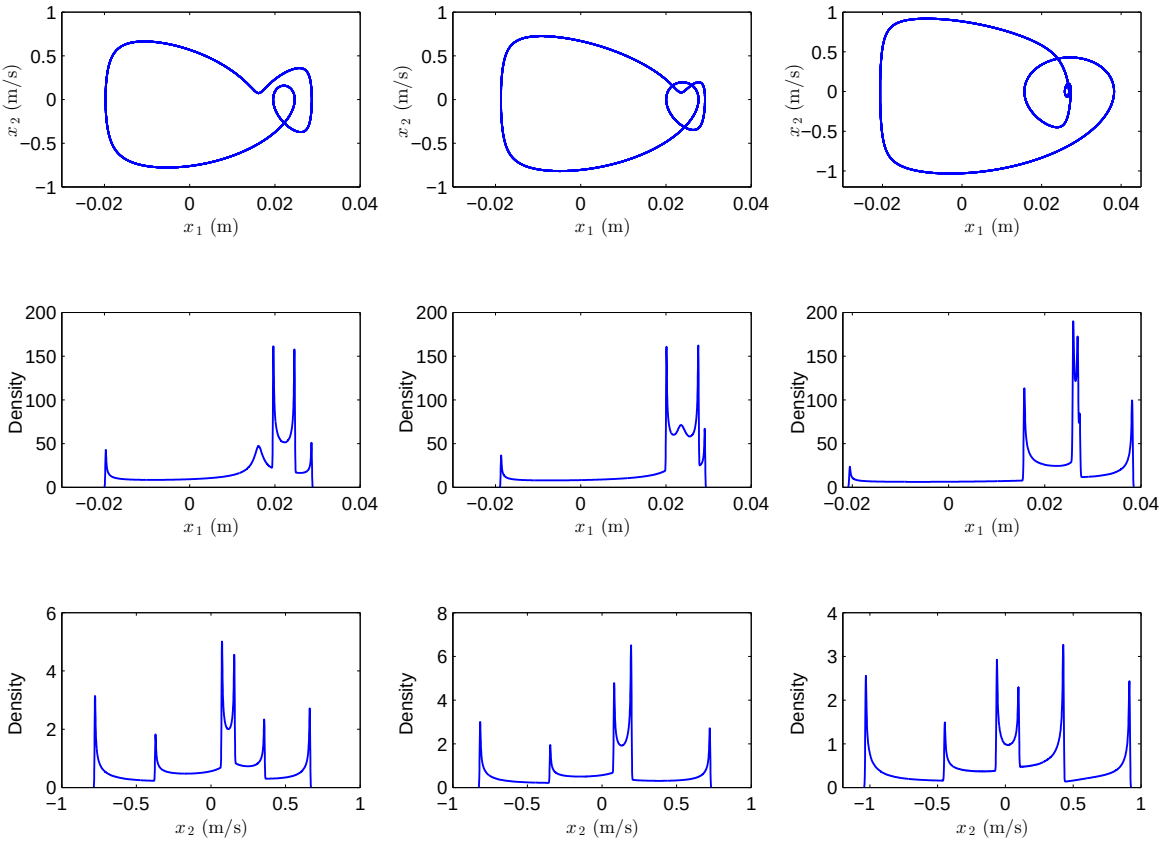

Figure 3. Sample phase portraits of the first mass and the corresponding probability density plots for x_1 and $\dot{x_1}$ time series

tem and computation of the response features each time. A total number of N=200 sample data were used to train, and validate the neural network.

Figure 4a shows the learning curve of the ANN for training, validation and test sets. The mean square error (MSE) can be seen as an index of the performance of the feature extraction

Table 2. Parameter values for three sample cases

	m_1 (kg)	m_2 (kg)	m_3 (kg)	r_{01} (m)	r_{02} (m)	r_{03} (m)
(a)	0.96	0.85	0.94	0.0207	0.0212	0.0220
(b)	0.98	0.85	0.91	0.0220	0.0200	0.0228
(c)	0.82	0.88	0.99	0.0223	0.0206	0.0211

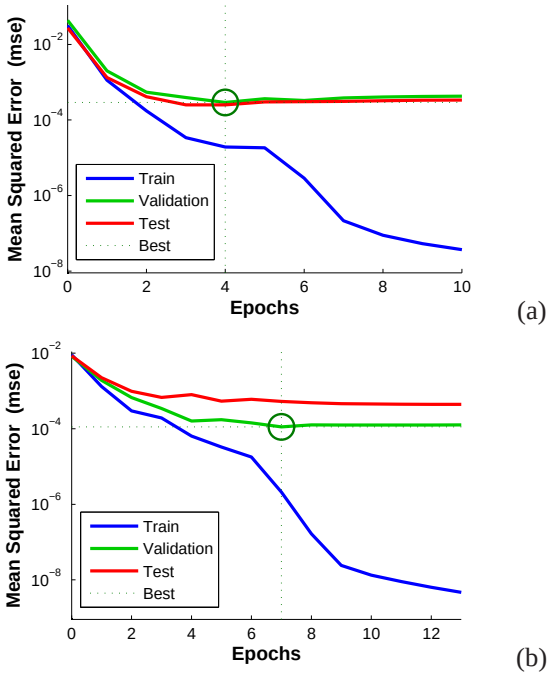

Figure 4. Learning curve of the neural network for training, validation, and test sets

and response characterization as lower values of MSE represent higher precisions in mapping the response features to the parameters sets. The best validation performance is achieved at epoch 35 with mean square error (MSE) of 1.3077×10^{-4}. The small values of MSE for all data sets are representatives of a perfect fit and effectiveness of the proposed method.

In real applications, some states of the system might not be available. For example in our system, we can only measure the position signals x_1, x_3 and x_5. We are interested to see how effective the method of PST would be when the whole phase space is not available. A new ANN was developed using the same data set; but only based on the features extracted from these three states. Figure 4b shows the MSE of the new ANN for training, validation and test sets. Interestingly, it can be seen that even though the convergence has taken a bit longer here, the minimum MSEs achieved here for all data sets are lower compared to the case where all six states were used. This can be due to the fact that a less number of inputs are involved in the optimization process which makes it computationally more efficient. This example clearly shows that including all states of the system does not necessarily provide additional information and make the analysis more efficient and accurate.

Estimation of Parameters

Figure 5 shows the estimated values of each parameter versus their real values for seventy cases, where all six parameters have been chosen randomly. Red points on this plot represent the estimated values of the real parameters on the set-up computed with experimental data. In order to do so, x_1, x_3 and x_5 were measured for these six random cases, and the corresponding features were extracted from them. As long as the obtained response is close enough to the response predicted by the mathematical model, the extracted features and the corresponding estimated parameters are expected to be close to their actual values. Figure 5 shows that the developed network can effectively estimate the values of m_1, m_2, and m_3; whereas the estimation error for r_{01}, r_{02} and especially r_{03} is relatively higher. Figure 6 shows the distribution of this estimation error for all six parameters. Note that in our analyses, all six parameters of the system were changed randomly at the same time, which rarely happens in real applications and makes the estimation problem more complicated.

4. CONCLUSION

A new method, namely the method of Phase Space Topology (PST) was employed in this paper to diagnose a multi degree of freedom system. The diagnostics was treated as a parameter estimation here, which is an accurate assumption for most real world defects. The features extracted from the nonlinear response of the system using PST are able to quantify the topology of the phase space trajectory. This is done by mapping the phase space trajectory into the density distribution plots of each state. The properties of the peaks in the density plots including their location, height and sharpness can describe this topology with quantitative measures.

The results show the effectiveness of the approach in characterizing the system behaviour and tracking the dynamical changes in the worst case scenario where six parameters were changed simultaneously. This is analogous to a system with six simultaneous defects which rarely happens in practice. The method shows superior capability in extracting useful information from the response in comparison to conventional

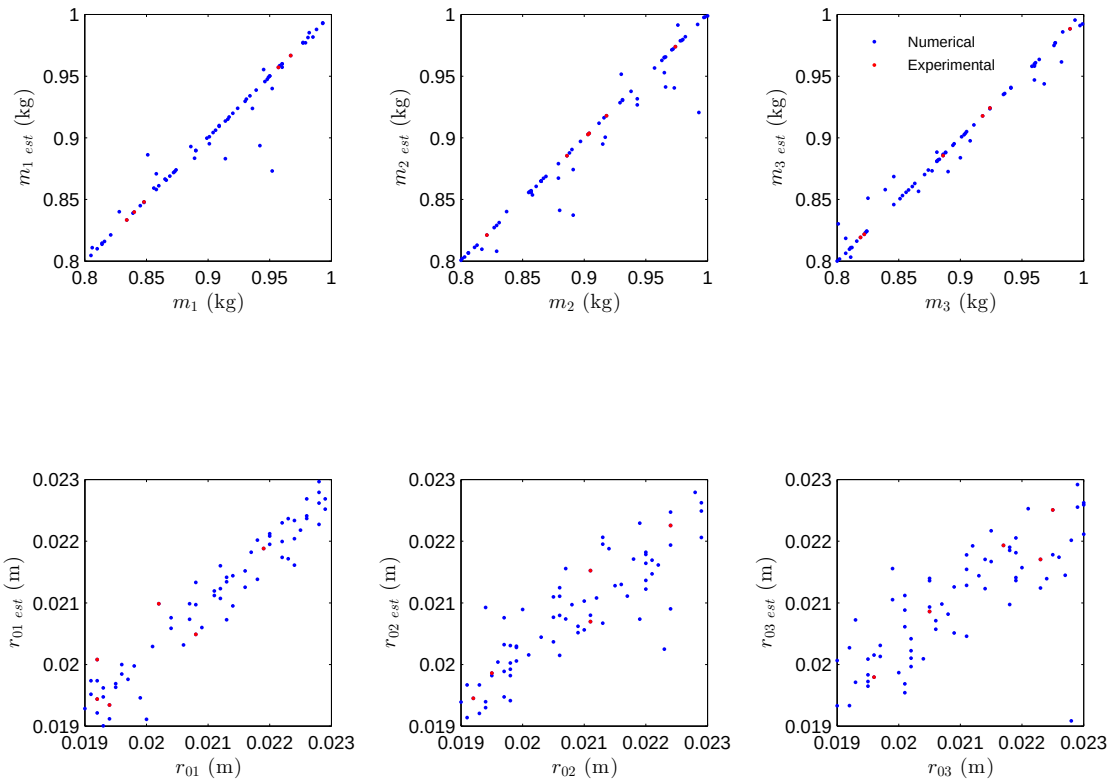

Figure 5. Estimated parameters for numerical and experimental data versus actual values

frequency, or time-frequency feature extraction methods which provide little information in the presence of nonlinear phenomena.

Some key aspects of the approach need to be addressed in the future work including the dependence of the method on density estimation parameters and robustness of the method to noise and other properties of data. The signals in this problem were fairly smooth and clean; whereas, in some real applications, the data is contaminated with noise and other uncertainties which makes the problem more complicated.

Acknowledgments

This work is supported by the US Office of Naval Research under the grant ONR N00014-13-1-0485. We deeply appreciate this support. Thanks are due to Mr Anthony Seman III of ONR.

REFERENCES

Carroll, T. (2015). Attractor comparisons based on density. *Chaos: An Interdisciplinary Journal of Nonlinear Science*, *25*(1), 013111.

Fekrmandi, H. (2015). Development of new structural health monitoring techniques.

Kappaganthu, K., & Nataraj, C. (2011). Nonlinear modeling and analysis of a rolling element bearing with a clearance. *Communications in Nonlinear Science and Numerical Simulation*, *16*(10), 4134-4145.

Letellier, C., Le Sceller, L., Dutertre, P., Gouesbet, G., Fei, Z., & Hudson, J. (1995). Topological characterization and global vector field reconstruction of an experimental electrochemical system. *The Journal of Physical Chemistry*, *99*(18), 7016–7027.

Mevel, B., & Guyader, J. L. (1993). Routes to chaos in ball bearings. *Journal of Sound and Vibration*, *162*(3), 471-487.

Rezvanizaniani, S. M., Dempsey, J., & Lee, J. (2014). An ef-

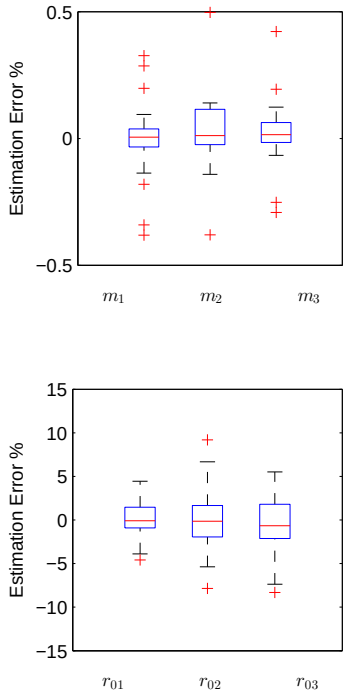

Figure 6. Distribution of estimation errors

fective predictive maintenance approach based on historical maintenance data using a probabilistic risk assessment: PHM14 data challenge. *International Journal of Prognostics and Health Management*.

Samadani, M., Kwuimy, C. K., & Nataraj, C. (2015). Model-based fault diagnostics of nonlinear systems using the features of the phase space response. *Communications in Nonlinear Science and Numerical Simulation*, *20*(2), 583–593.

Sankaravelu, A., Noah, S. T., & Burger, C. P. (1994). Bifurcation and chaos in ball bearings. *ASME Applied Mechanics Division-publications*, *192*, 313-313.

Tufillaro, N., Holzner, R., Flepp, L., Brun, E., Finardi, M., & Badii, R. (1991). Template analysis for a chaotic NMR laser. *Physical Review A*, *44*(8), R4786.

BIOGRAPHIES

Mohsen Samadani Mohsen received his B.Sc and M.Sc in Mechanical Engineering from Isfahan University of Technology, Isfahan, Iran. He is currently a Ph.D. candidate at the Department of Mechanical Engineering at Villanova University. Mohsen has been involved in various research topics including manufacturing technologies, control, vibrations, system dynamics, hydraulic systems and reliability analysis. His current research interests include data analysis, machine learning, nonlinear dynamics and vibrations with applications to machinery diagnostics and health management. He is a member of Sigma Xi and ASME and a recipient of Sigma Xi best poster award and PHM doctoral consortium travel award.

Cedrick Kwuimy Prior to joining the Department of Mechanical Engineering at Villanova University in Jan. 2011, Dr. Kwuimy worked in South Africa as a postdoctoral research associate at the African Institute for Mathematical Sciences (2009-2010) and as a Research and Teaching Assistant (2007-2009) at the Faculty of Science at the University of Yaounde, Cameroon. He has been involved in a wide range of research topics including vibration control, nonlinear dynamics of self-sustained electromechanical devices, synchronization, nonlinear analysis of butterfly valves, and chaos control and prediction in active magnetic bearings. He has over 30 peer-reviewed papers in international journals and conference proceedings and serves as a reviewer in high standard journals including Nonlinear Dynamics, Journal of Vibration and Control and Journal of Sound and Vibration. Dr. Kwuimy has supervised three graduate research theses at the African Institute for Mathematical Sciences and is the recipient of Victor Rothschild Fellowships at African Institute for Mathematical Sciences and Research.

C. Nataraj Dr. C. Nataraj holds the Mr. and Mrs. Robert F. Mortiz, Sr. Endowed Chair Professorship in Engineered Systems at Villanova University. He has a B.S. in Mechanical Engineering from Indian Institute of Technology, and M.S. and Ph.D. in Engineering Science from Arizona State University. After getting his Ph.D. in 1987, he worked for a year as a research engineer and a partner with Trumpler Associates, Inc. He is currently the Chairman of the Mechanical Engineering Department at Villanova University. Dr. Nataraj was also the founding director of the Center for Nonlinear Dynamics and Control in the College Of Engineering. He has worked on various research problems in nonlinear dynamic systems with applications to mobile robotics, unmanned vehicles, rotor dynamics, vibration, control, and electromagnetic bearings. His research has been funded by Office of Naval Research, National Science Foundation, National Institute of Health and many companies.